ACS APPLIED MATERIALS & INTERFACES

Research Article

www.acsami.org

Poly(methyl methacrylate)/Graphene Oxide Layered Films as Generators for Mechanical Energy Harvesting

Luca Valentini,*[,†] Silvia Bittolo Bon,[†] and Josè M. Kenny[†,‡]

[†]Dipartimento di Ingegneria Civile e Ambientale, Università di Perugia, Strada di Pentima 4, INSTM, UdR Perugia, 05100 Terni Italy

[‡]Instituto de Ciencia y Tecnologia de Polimeros, CSIC, Juan de la Cierva, 3, 28006 Madrid, Spain

Supporting Information

ABSTRACT: In this work we introduce a simple practical way to transfer large flakes of partially reduced graphene oxide (rGO) as well as poly(methyl methacrylate)/rGO films onto arbitrary substrates where the electrode geometry is defined before the film deposition to fabricate devices. It was reported how such films when stimulated by an ultrasound transducer convert mechanical energy to electricity. The possibility to utilize polymer nanocomposites as nanogenerators is of current interest to enhance mechanical energy harvesting and to add new functionalities to polymer nanocomposites.

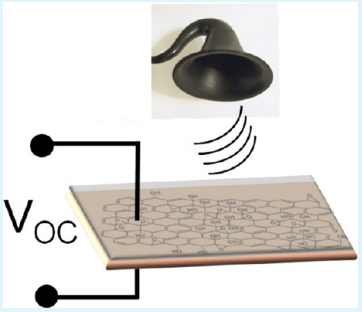

KEYWORDS: *graphene oxide, polymer nanocomposite, thin films, electrical properties, energy harvesting*

1. INTRODUCTION

Sound generated above the human hearing range (typically 20 kHz) is called ultrasound. Although ultrasound behaves in a similar manner to audible sound, it has a much shorter wavelength. This means it can be reflected off very small surfaces. The boundary between two materials of different acoustic impedances is called an acoustic interface. When sound strikes an acoustic interface at normal incidence, some amount of sound energy is reflected and some amount is transmitted across the boundary.

Harvesting such mechanical energy, an important energy resource, directly from the environment has been proposed as an effective approach to powering nanodevices.[1,2] Numerous piezoelectric nanomaterials have been investigated as generators of electricity, such as zinc oxide and indium nitride nanowires, lead zirconate titanate, and poly(vinylidene fluoride) nanofibers.[3−6]

Recently, strain engineering of the electronic properties of graphene, a one-atom thick two-dimensional molecule made of sp^2 hybridized carbon atoms, which can be described through the generation of local magnetic fields by strain,[7−10] has attracted considerable attention. Most recently monolayer graphene grown on copper by chemical vapor deposition (CVD) was used to demonstrate thermoacoustic sound generation.[11] Ruoff et al.[11] used the physical approach of applying an alternating current to a conductor, i.e. graphene sheet, that heats the conductor, resulting in a variation of the air density, which causes pressure oscillations (i.e., sound waves).

The main drawback of this approach is the deposition method adopted for obtaining a monolayer of graphene; generally single-layer graphene sheets are prepared by mechanical exfoliation,[12] epitaxial growth,[13] and chemical methods.[14] Furthermore, the high cost of single crystal substrates and the ultra high vacuum conditions necessary for growth significantly limit the use of these methods for large scale applications.

Among these methods, the most common route toward large quantities of reduced graphene begins with the oxidation of graphite to graphene oxide (GO). The oxidation of graphite to GO breaks the sp^2 hybridized structure generating defects that increase the distance between adjacent sheets from 0.335 nm in graphite to 0.68 nm for GO powder.[15−17] This increased spacing as well as the presence of hydrophilic functional groups reduces interaction between sheets, thus facilitating the delamination of GO into single layer graphene oxide sheets upon exposure to water in a sonication bath. GO sheets positively charged because of H^+ charge trapping through oxygen-containing functional groups have been integrated into nanogenerators for harvesting acoustic energy.[18] The fabrication of the nanogenerator requires the integration of suspended GO sheets between electrodes consisting of poly(3,4-ethylenedioxythiophene) poly(styrenesulfonate) and Al membrane. However, some of these approaches require the use of a specific substrate material.

Graphite, the raw material for producing solution processed graphene, is cheap (~$1275−1700/ton) and abundant. The subsequent processing needed to produce solution-processable graphene leads to an estimated cost of GO based only on the price of raw materials used in Hummer's methods of about 10−20 times that of graphite. Thus, films derived from liquid

Received: January 29, 2013
Accepted: April 15, 2013
Published: April 15, 2013

   dx.doi.org/10.1021/am400388f | ACS Appl. Mater. Interfaces 2013, 5, 3770−3775

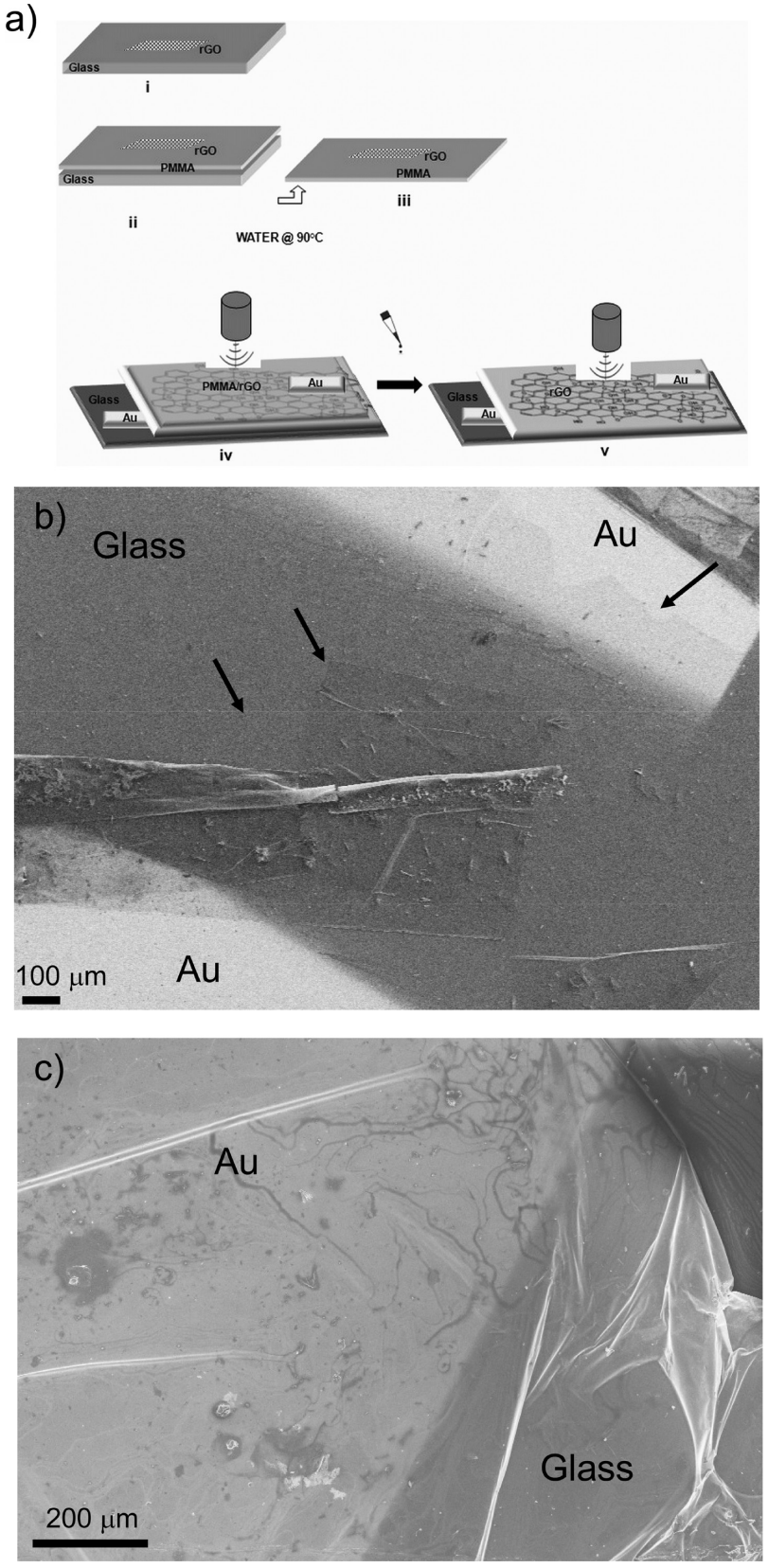

Figure 1. (a) Schematic diagram of the steps for the fabrication of the device: (i) GO flakes were deposited by drop casting and thermally reduced (rGO); (ii) the PMMA was spin-cast onto rGO coated glass substrate; and (iii) the rGO flakes embedded in the PMMA matrix were detached from the native substrate by immersion in water at 90°C. (iv) Transferring of freestanding layered film with tweezers on the target substrate and testing under an acoustic transducer. (v) Testing of rGO flakes under an acoustic transducer after dissolving the PMMA with acetone and isopropanol. (b) FESEM image of rGO sheet deposited on glass between the Au electrodes. The arrows serve to the eyes to visualize rGO sheets. (c) High magnification view of rGO sheet near the Au electrode.

dx.doi.org/10.1021/am400388f | ACS Appl. Mater. Interfaces 2013, 5, 3770−3775

suspensions of graphene flakes can potentially overcome these limitations. The main issue of this work deals with the electrical response to ultrasounds of GO sheets immobilized between two electrodes via polymer transfer method. Here, in analogy to the widespread use of traditional piezoelectric materials, we report the proof-of-concept on the use of polymer/graphene oxide layered film as nanogenerator for mechanical energy harvesting via a simple solution-based deposition method.

2. EXPERIMENTAL DETAILS

Graphene oxide were purchased from Cheaptubes (thickness 1-5 nm estimated by AFM[19]). Water dispersion (1 mg/mL) was prepared and tip sonicated (750W, 60% amplitude) for 1 h to yield a yellow suspension. After this mixing process, the solution was transferred to a vial, and it was centrifuged for 30 min at 9000 rpm. Quartz substrates (20 mm × 20 mm; 1 mm thick) were cleaned by ethanol and acetone, rinsed with water, dried under nitrogen, and taken inside a dry Ar glove box. Graphene oxide films were prepared by spreading the GO water solution onto the glass substrates. The deposited films were then annealed at 400°C for 4 h in vacuum (10^{-3} Torr) to get partially reduced GO (rGO). The infrared spectra of the deposited film were recorded in transmission mode between 250 and 3500 cm^{-1} (see the Supporting Information).

Poly(methyl methacrylate) (PMMA, average $M_w \approx 996\,000$, T_g = 125 °C) was purchased from Sigma Aldrich. PMMA was spin-cast (4% in anysole) on top of the glass coated with rGO at 1000 rpm for 1 min. After that, the sample was soaked at 90 °C in DI water until the complete detachment of the PMMA film because of the hydrophobic nature of the polymer film and the hydrophilic one of the GO. The floating film is moved on top of the target substrate. For the device fabrication, the detached film consisting of partially reduced GO flakes embedded in the polymer matrix was moved onto metal electrode, which were made up of Au that were previously deposited onto a glass substrate by vacuum evaporation (0.01 Pa) with an optimized thickness of 60 nm. The top electrode array (4 mm × 4 mm) was deposited subsequently by vacuum evaporation.

Raman spectroscopy was conducted using a Bruker Dispersive Raman spectrometer with 532 nm Nd:YAG laser. A maximum laser power of 3 mW was applied on three different points of each sample for 30 s of accumulation time. FESEM and TEM analyses were performed with a Zeiss-Supra25 and Philips EM 400 instruments, respectively.

For the device fabrication, the detached film consisting of reduced GO flakes embedded in the polymer matrix was moved onto metal electrodes, which were made up of Au and spaced 1 mm that were previously deposited onto a glass substrate by vacuum evaporation (10^{-4} Torr) with an optimized thickness of 60 nm. The deposited films were then annealed at 100 °C for 1 h to evaporate trapped water. A device consisting of partially rGO flakes was also realized by removing the PMMA matrix by washing in acetone for 2 min and then in isopropanol for 1 min. Figure 1a shows a schematic illustration of the successive steps followed for the device fabrication.

A contact transducer generating a longitudinal acoustic wave of 2 MHz was put in direct contact with the top of the freestanding film. Transducer waveform and spectrum analysis is done according to test conditions and definitions of ASTM E1065. The acoustic wave was also generated onto the device layout without the material between the electrodes in order to record any electrical signal generated from the acoustic interference with the glass substrate (see the Supporting Information). The output current from the electrodes was collected at room temperature with a Keithley 4200-SCS semiconductor analyzer. The output current was recorded by applying a bias voltage between 10 and 20 V to the gold electrodes. The short circuit current signal was recorded in a common voltage bias configuration.

3. RESULTS AND DISCUSSION

Figure 1b and c show FESEM images of partially rGO flakes, deposited by mechanical transfer method illustrated in Figure 1a after the removal of PMMA, between the gold electrodes. The images show large flakes with wrinkled and folded regions (Figure 1c).

Raman spectrum of the flakes shown in Figure 1b is reported in Figure 2a. In particular the G band at ~1579 cm^{-1}, the 2D band at ~2716 cm^{-1}, and the disorder-related D peak at ~1350 cm^{-1} are evident. Figure 2b shows a symmetric 2D peak with wavelength and shape similar to that of bi-layer grapheme.[20] Moreover the high intensity of the disorder related D peak, accordingly to Ferrari et al.,[20] is attributed to the edges of the micrometer size flakes as reported in Figure 1b. Raman analysis provides further insight into the number of layers and structural changes of the graphene flakes in terms of exfoliation of drop cast GO flakes induced by the removal of the PMMA coating. The disappearance of the second-order zone boundary phonon (2D), observed for the drop cast GO, confirms the layering induced by the polymer transfer (see the Supporting Information).

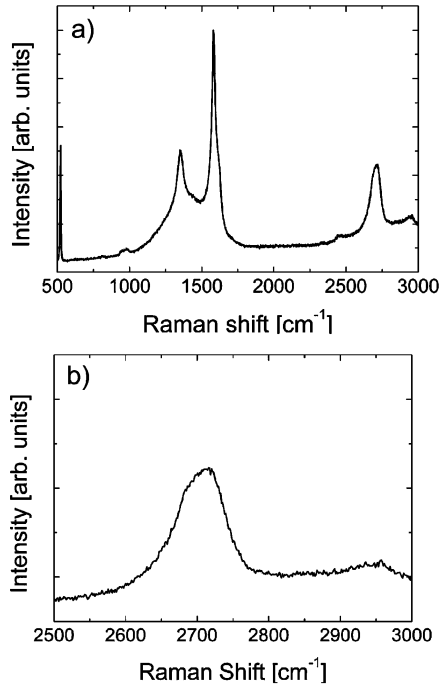

Figure 2. (a) Raman spectrum of rGO film. (b) Enlargement of the 2D Raman region of rGO film.

The easy processing and the versatile properties of GO make the thermal reduction method for such material one of the most attractive way for partially restoring the charge carrier transport. Recently, it has been shown that deoxygenation occurs in GO when it is heated above 100 °C,[21] resulting in a thermal reduction.

The current−voltage characteristics of the prepared samples were investigated. The low conductivity of GO (Figure 3a) is due to the existence of oxygen-containing groups, which introduce defects to graphene.[21] The partial GO deoxygenation (see the Supporting Information) after the thermal treatment increases, as expected, its conductivity to some extent (Figure 3a).

A transducer is any device that converts one form of energy to another. An ultrasonic transducer converts electrical energy to mechanical energy, in the form of sound. Being a one-atom-thick structure, it is reasonable to predict that strain can

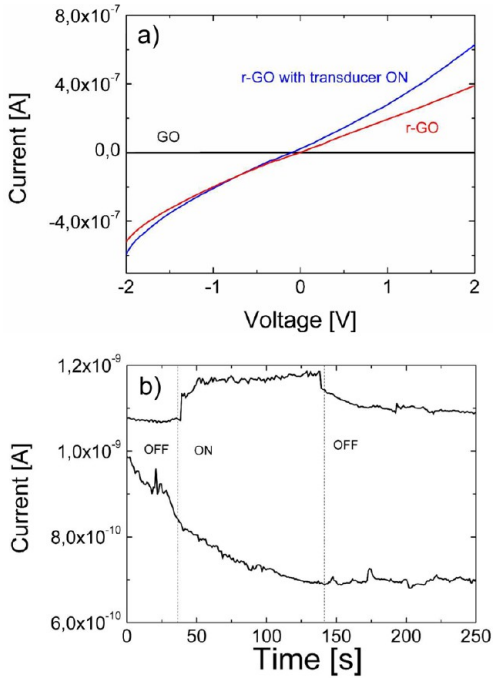

Figure 3. (a) $I-V$ characteristics of GO (black), rGO (red) with the transducer turned off and rGO (blue) with the transducer turned on. (b) Current of GO (bottom) and rGO (top) devices with the transducer turned off and on, respectively.

dramatically modify the electronic and optical properties of graphene. In particular, recent experiments[22,23] have demonstrated that graphene single layer can reversibly sustain elastic deformations as large as 20% as well as it shows strain-induced modifications of the electronic and transport properties.[23]

In this regard, Figure 3a compares the current/voltage characteristics of the device consisting of rGO film when the acoustic transducer schematized in Figure 1a was switched on. It is evident how, the device made from reduced GO, responded to acoustic vibration generating current. In order to check if this effect is reversible the current before and after one cycle of ultrasounds was monitored (Figure 3b).

As for the voltage sweep measurements also in this case the variation of the current was recorded only for the device fabricated with partially rGO film while any current variation was observed for the GO film when the transducer was turned on. It is interesting also to observe for the rGO sample a quasi-reversible effect of the current generation. The difference of the current values of rGO device in Figure 3a and b was due to the different distance between the electrodes for the two measurements.

As stated above the proposed transferred method allows us to locate in a precise position and, more importantly, at any fabrication step freestanding films circumventing processing steps (chemical etching, temperature, e-beam lithography) which can be destructive for the graphene flakes. In this way, we are able to fabricate all the devices which require freestanding films. Figure 4a shows the photograph of the partially rGO embedded onto the PMMA matrix after the film detachment from native glass substrate and its transferring on top of the Au electrodes. The TEM analysis of the PMMA/rGO sample reveals large and folded flakes (Figure 4b).

Graphene oxide is a water-soluble insulating material, which combined with polymer matrices could meet the technological challenges for delivering low-cost and thin dielectric composite materials that exhibit a relatively high dielectric constant with a small loss factor to be used both as resistive and capacitive field grading materials.

The mean current for the PMMA/rGO sample was lower than for rGO film (Figure 3b), indicating that the PMMA/rGO film contained fewer charges (Figure 4c). In polymer composite containing GO, the electric charges are either forced to take a more circuitous route or completely constrained in narrow spaces inside the polymer matrix.[24] Thus the current drops quickly as charges encounter the polymer, and the conductivity of the composite is several orders of magnitude lower than that of the rGO film.

Figure 4c illustrates the correlation between the acoustic signal and the output mean currents. The results demonstrate that also for the layered film, the acoustic wave generates a reversible electric signal with a variation of about 5% with respect to the base signal. Under the agitation of the acoustic wave, the mean distance between the rGO flakes and polymer chains changes inducing a charge density to form a current in between the two electrodes. In order to provide the proof on the piezoelectricity of the fabricated materials, we investigated if the electrical output was simply due to the change of resistance of the composite (Figures 4d–e).

PMMA is ideal for assisting graphene transfer due to the strong dipole interactions between PMMA and chemical groups on graphene resulting in long chain molecules sticking to the graphene.[25] Therefore, the distance variation of the electric dipole induced by the acoustic wave results in a transient current due to the charge redistribution on the gold electrodes to produce a steady state between the external and internal electric field of the PMMA/rGO dielectric, respectively.

It is also evident that when the acoustic wave strikes the sample, a short circuit current variation (i.e. common voltage bias) (Figure 4d) was observed. It is also evident that when the transducer was switched on we observed a built-in voltage along with a short circuit voltage generating an output power (Figure 4e). The output electrical power from the device is $IV = 3.90 \times 10^{-10}$ W. The input sound power to the device is 2×10^{-9} W. Therefore, the conversion efficiency to electrical energy is $3.90 \times 10^{-10}/(2 \times 10^{-9}) = 19.5\%$.

It should be mentioned that ultrasound used in this experiment is a regular periodic mechanical energy, however in the natural environment, the frequency fluctuates a lot. Details of acoustic impact responses stimulated by falling water droplets arriving at the surface of our freestanding films are an area of research that is under investigation in our lab. These considerations will be important for development of the technique on concrete structures in this field.

4. CONCLUSIONS

We introduce a clean practical way to transfer large flakes of partially reduced graphene oxide as well as PMMA/GO films onto arbitrary substrates. The water-based process has been proven to deposit few layer rGO film, as confirmed by Raman spectroscopy. The technique has been shown to allow the fabrication of devices, such a nanogenerators, with electrodes defined before the rGO deposition. Partially reduced GO flakes embedded onto a PMMA film can convert the acoustic energy into electricity. Such low-cost, easily processed, and flexible nanogenerators are promising candidates for acoustic energy harvesting.

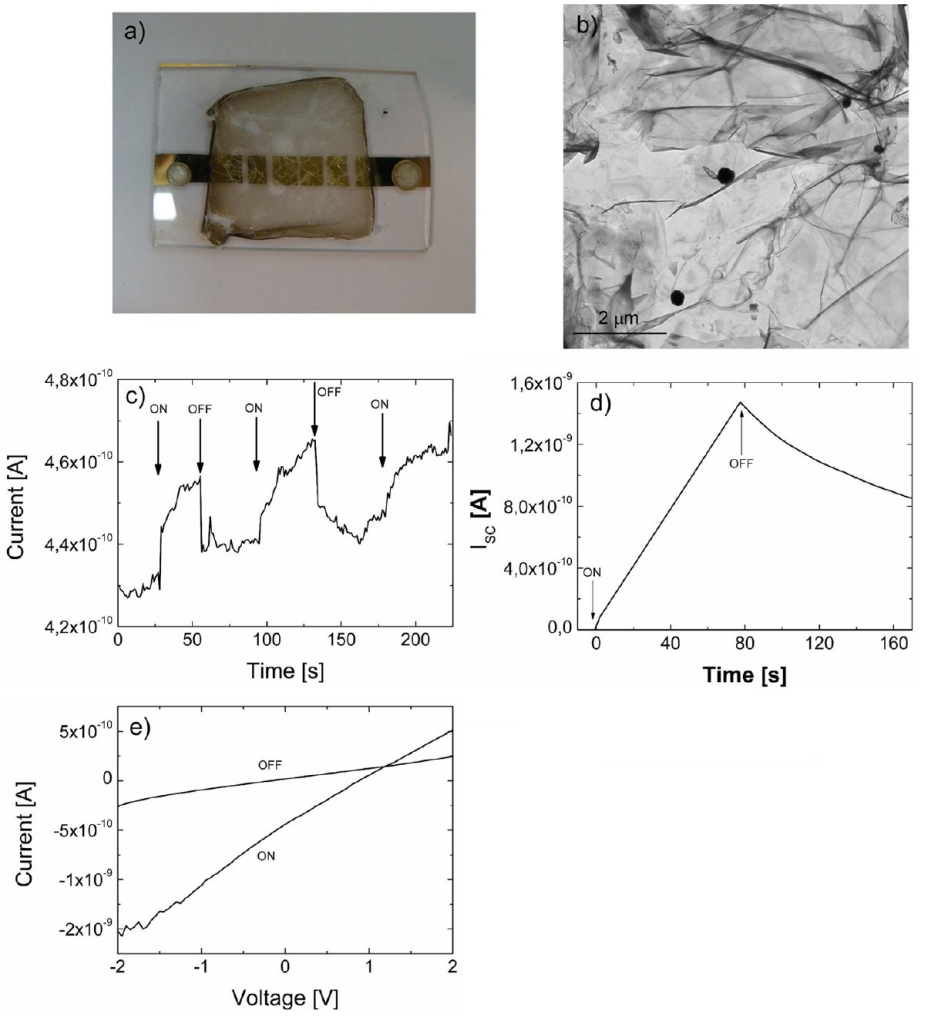

Figure 4. (a) Photograph of PMMA/rGO film deposited on glass between the Au electrodes. (b) TEM image of PMMA/rGO sample. (c) Current of PMMA/rGO device versus acoustic transducer vibration. (d) Short circuit electrical current of PMMA/rGO film recorded with the transducer turned on and off, respectively. (e) Current–voltage curves of PMMA/rGO device with the transducer turned off and on, respectively.

■ ASSOCIATED CONTENT

Supporting Information

Figures S1–S3. This material is available free of charge via the Internet at http://pubs.acs.org.

■ AUTHOR INFORMATION

Corresponding Author

*Tel.: +39-0744-492924. E-mail: mic@unipg.it.

Notes

The authors declare no competing financial interest.

■ REFERENCES

(1) Huang, C. T.; Song, J. H.; Lee, W. F.; Ding, Y.; Gao, Z.; Hao, Y.; Chen, L. J.; Wang, Z. L. *J. Am. Chem. Soc.* **2010**, *132*, 4766–4771.
(2) Xu, S.; Qin, Y.; Xu, C.; Wei, Y.; Yang, R.; Wang, Z. L. *Nat. Nanotechnol.* **2010**, *5*, 366–373.
(3) Wang, Z. L.; Song, J. *Science* **2006**, *312*, 242–246.
(4) Huang, C. T.; Song, J.; Tsai, C. M.; Lee, W. F.; Lien, D. H.; Gao, Z.; Hao, Y.; Chen, L. J.; Wang, Z. L. *Adv. Mater.* **2010**, *22*, 4008–4013.
(5) Chen, X.; Xu, S.; Yao, N.; Shi, Y. *Nano Lett.* **2010**, *10*, 2133–2137.
(6) Chang, C.; Tran, V. H.; Wang, J.; Fuh, Y. K.; Lin, L. *Nano Lett.* **2010**, *10*, 726–731.
(7) Fogler, M. M.; Guinea, F.; Katsnelson, M. I. *Phys. Rev. Lett.* **2008**, *101*, 226804.
(8) Guinea, F.; Katsnelson, M. I.; Geim, A. K. *Nat. Phys.* **2010**, *6*, 30–33.
(9) Levy, N.; Burke, S. A.; Meaker, K. L.; Panlasigui, M.; Zettl, A.; Guinea, F.; Neto, A. H. C.; Crommie, M. F. *Science* **2010**, *329*, 544–547.
(10) Kim, K.-J.; Blanter, Y.; Ahn, M. K-H. *Phys. Rev. B* **2011**, *84*, 081401.
(11) Suk, J. W.; Kirk, K.; Hao, Y.; Hall, N. A.; Ruoff, R. S. *Adv. Mater.* **2012**, *24*, 6342–6347.
(12) Novoselov, K. S.; Geim, A. K.; Morozov, S. V.; Jiang, D.; Zhang, Y.; Dubonos, S. V.; Grigorieva, I. V.; Firsov, A. A. *Science* **2004**, *306*, 666–669.
(13) Berger, C.; Song, Z.; Li, X.; Wu, X.; Brown, N.; Naud, C.; Mayou, D.; Li, T.; Hass, J.; Marchenkov, A. N.; Conrad, E. H.; First, P. N.; de Heer, W. A. *Science* **2006**, *312*, 1191–1196.
(14) Liu, N.; Luo, F.; Wu, H.; Liu, Y.; Zhang, C.; Chen, J. *Adv. Funct. Mater.* **2008**, *18*, 1518–1525.
(15) Park, S.; Ruoff, R. S. *Nat. Nanotechnol.* **2009**, *4*, 217–224.
(16) Park, S.; An, J.; Jung, I.; Piner, R. D.; An, S. J.; Li, X.; Velamakanni, A.; Ruoff, R. S. *Nano Lett.* **2009**, *9*, 1593–1597.
(17) Stankovich, S.; Dikin, D. A.; Piner, R. D.; Kohlhaas, K. A.; Kleinhammes, A.; Jia, Y.; Wu, Y.; Nguyen, S. T.; Ruoff, R. S. *Carbon* **2007**, *45*, 1558–1565.

(18) Que, R.; Shao, Q.; Li, Q.; Shao, M.; Cai, S.; Wang, S.; Lee, S.-T. *Angew. Chem. Int. Ed.* **2012**, *51*, 5418−5422.
(19) Bittolo Bon, S.; Valentini, L.; Kenny, J. M. *Chem. Phys. Lett.* **2010**, *494*, 264−268.
(20) Ferrari, A. C.; Meyer, J. C.; Scardaci, V.; Casiraghi, C.; Lazzeri, M.; Mauri, F. *Phys. Rev. Lett.* **2006**, *97*, 187401−187403.
(21) Eda, G.; Chhowalla, M. *Adv. Mater.* **2010**, *22*, 2392−2415.
(22) Kim, K. S.; Zhao, Y.; Jang, H.; Lee, S. Y.; Kim, J. M.; Kim, K. S.; Ahn, J. H.; Kim, P.; Choi, J.; Hong, B. H. *Nature* **2009**, *457*, 706−710.
(23) Ni, Z. H.; Yu, T.; Lu, Y. H.; Wang, Y. Y.; Feng, Y. P.; Shen, Z. X. *ACS Nano* **2008**, *2*, 2301−2305.
(24) Stauffer, D.; Aharony, A. In *Introduction to Percolation Theory*, 2nd ed.; Taylor & Francis: London, 1992.
(25) Li, X.; Zhu, Y.; Cai, W.; Borysiak, M.; Han, B.; Chen, D.; Piner, R. D.; Colombo, L.; Ruoff, R. S. *Nano Lett.* **2009**, *9*, 4359−4363.